ELSEVIER

Separation and Purification Technology 30 (2003) 201–214

Separation and Purification Technology

www.elsevier.com/locate/seppur

Monte Carlo simulation on the concentration distribution of non-spherical particles in cylindrical pores

Ik-Tae Im [a,*], Myung-Suk Chun [b]

[a] *Department of Automotive Engineering, Iksan National College, 194-5, Ma-dong, Iksan, Jollabuk-do 570-752, South Korea*
[b] *Polymer Division, Membranes Laboratory, Korea Institute of Science and Technology, P.O. Box 131, Cheongryang, Seoul 131-650, South Korea*

Received 11 March 2002; received in revised form 23 July 2002; accepted 23 July 2002

Abstract

Partition coefficients and concentration profiles of rigid, non-spherical, axisymmetric particles between bulk solution and cylindrical pores have been calculated by stochastic Gibbs ensemble Monte Carlo (GEMC) simulation. The element spheres are used to describe the axisymmetric, non-spherical particles. The method of element spheres for describing the particles shows remarkable reduction of computational times. Developed Monte Carlo simulation method can be applied to calculate the equilibrium partitioning of the high volume concentration solution that cannot be solved analytically. The simulation results show that solute density is higher near the pore wall than the pore center. In the case of high concentration, the solute density in the pore is highly dependent upon the bulk solution concentration. And the partition coefficient, K increases with increasing of the aspect ratios and bulk solution concentrations.

Keywords: Partitioning coefficient; Concentration profile; Monte Carlo method; Non-spherical particles

1. Introduction

The equilibrium partitioning of rigid particles between a bulk solution and an adjacent porous solids, and the concentration profile in pores are important aspects of hindered diffusion and related topics, such as membrane filtration process, gel permeation chromatography and a transport process in biology. Within a pore, the interstitial space of a solid porous material, the concentration is partitioned due to the steric interactions of particle to pore wall and/or particle-to-particle interactions. If the particles and pore walls are electrically charged, the interactions become more sophisticated.

The partition coefficient K can be defined as the ratio of mean pore-to-bulk concentration at equilibrium:

* Corresponding author. Tel.: +82-63-840-6651
E-mail address: itim@iksan.ac.kr (I.-T. Im).

1383-5866/02/$ - see front matter
PII: S1383-5866(02)00143-0

Nomenclature

a	length of semi-minor axis of a spheroid
b	length of semi-major axis of a spheroid
C	solute concentration of the ith shell
C_b	solute concentration in the bulk
C_p	solute concentration in the pore
d	distance, Eqs. (6) and (7)
E_α	interaction energy of the subsystem α
E_β	interaction energy of the subsystem β
h	sum of radii, Eq. (6)
k	Boltzmann's constant
N_α	number of particles in the subsystem α
N_β	number of particles in the subsystem β
N_i	number of particles in the ith shell
n_d	number of element spheres in a particle
n_t	number of element spheres in the ith shell
p_D	probability of the NVT metropolis scheme, Eq. (3)
p_T	probability of the particle transfer between regions, Eq. (4)
R_i	inner radius of the ith shell
R_p	pore radius
r_s	radius of a element sphere
T	Temperature
V_α	volume of the subsystem α
(x, y, z)	global coordinate system
(x_0, y_0, z_0)	center position of a solute
(x', y', z')	solute-fixed coordinate system
Greek letters	
β	radial coordinate
γ	aspect ratio of a particle
λ	dimensionless characteristic length of a particle

$$K = \frac{C_p}{C_b} = \frac{\int_0^{1-\lambda} c(\beta)\beta \, d\beta}{\int_0^1 c(\beta)\beta \, d\beta} \quad (1)$$

where λ the non-dimensional characteristic length of the particle and β is the radial coordinates. In the limit of an uncharged infinite dilute solution, the effects of solute–solute interactions are negligible and only solute-pore wall interactions have to be considered. In this case, the partition coefficient shown in the above Eq. (1) exhibits the asymptotic behavior:

$$K = 1 - \lambda \quad (2)$$

as λ approaches zero. In the case of high concentration bulk solution, both of the particle-to-particle interactions and the particle-to-wall interactions have to be considered to find the partition coefficients.

Most of the previous researches on the partitioning of solid particles have been restricted to the sphere particles. The most extensive analysis on the partitioning of non-spherical particles was the seminal work of Giddings et al. (1). They established a general foundation for partitioning from the principles of statistical thermodynamics, and showed the partition coefficient for the non-spherical particles in various pores can be ex-

pressed as the ratio of the configurational integrals.

From the boundary perturbation method, Limbach et al. (2) have proposed the relatively simple equations for the partition coefficients of the various non-spherical particles including disc, rod, hemisphere, prolate and oblate spheroids. They also compared the perturbation analysis results with the Monte Carlo simulation. The results from the boundary perturbation analysis were in good agreement with the results from the Monte Carlo simulation even at rather large values of the ratio of molecule size to pore radius. Nitsche and Limbach (3) have driven an approximate formula for partition coefficients of non-axisymmetric, non-spherical solid molecules using a perturbation analysis. They compared the perturbation results with the Monte Carlo simulation results.

The above researches, however, are on the infinite dilute cases and have limitations to the real, high concentration solutions. Analytical approach of the partitioning behavior for the high concentration solution is very difficult because of the complex steric interactions of the particles. In this study, the partitioning behavior for the rigid, non-spherical, axisymmetric particles of high bulk solution concentration are analyzed by the Gibbs ensemble Monte Carlo (GEMC) simulations. The effects of steric interactions according to the particle shapes and aspect ratios on the partition coefficients, where the solute concentrations range up to 20 vol%, is investigated. Well-defined cylindrical pore, shown in the Fig. 1, is assumed and the thin rod-like and prolate spheroids are used as axisymmetric non-spherical particles due to the importance and simplicity of expression. Simulation results of partitioning behavior and concentration distribution can be used to estimate the hindered diffusion by considering the transport of non-spherical particles through the pores.

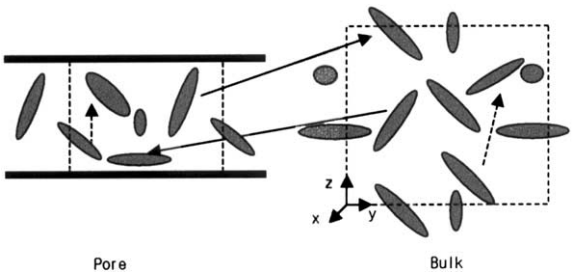

Fig. 1. GEMC method for the simulation of equilibrium partitioning of non-spherical particles between cylindrical pores and bulk solution, solid arrows depict the particle interchange and dotted arrows represent random particle moves.

2. Theories and numerical method

2.1. Monte Carlo method

The GEMC method is used to find the equilibrium partition coefficient in this study. In essence, the GEMC method is composed of four elements, canonical (NVT), isobaric–isothermal (NPT), and grand canonical (μVT) ensembles (4). The GEMC method allows one to simulate coexisting subsystems consisting of a pore region 'p' and a bulk region 'b' in equilibrium at a temperature T. To achieve this, pore and bulk regions are constructed having volumes V_p and V_b and containing N_p and N_b solute particles, respectively.

The two regions are allowed to interchange particles and the volumes are allowed to fluctuate in order to satisfy the equilibrium conditions of the temperature, pressure, and chemical potential μ. A complete cycle of the GEMC simulation generally consists of three types of moves. However, the pore–bulk system used in this study, there is no need to include exchanges of volume between the two regions (5). Therefore, only two types of moves, particle displacement within each region and interchange moves between regions are performed.

The unit computational cells for bulk and pore are a cube and a finite cylinder, respectively. The periodic boundary condition is used for the entire x, y, and z directions of a bulk unit and the axial direction of a cylindrical pore. The computational cells and concepts of random particle displacements in each region and particle interchange between the two regions are shown in the Fig. 1. The dotted lines are the unit cell boundaries at which the periodic boundary condition is imposed and the arrows explain the schematics of particle moves and interchanges.

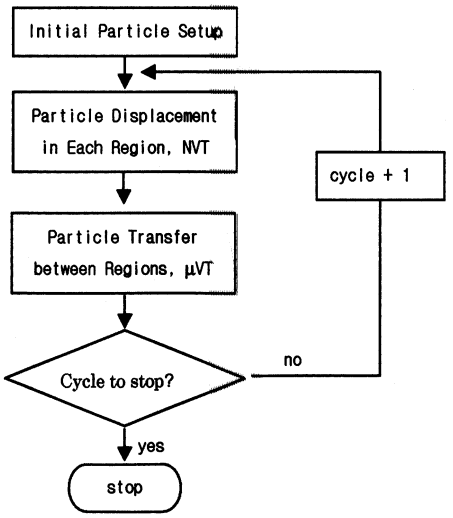

Fig. 2. Computational procedures of the GEMC simulation.

In the stage of the first type of move, the random displacement of particles in each subsystem, the particles are chosen and displaced randomly within the periodic unit cells following the NVT metropolis scheme (6). If the new configurations of particles after a random displacement are possible without the interactions among particles or pore wall such as overlap, the random displacement is adopted. If the displaced particle is overlapped with another particles or not permitted by the pore wall, the displacement is not allowed.

The probability p_D restricts the new configurations of the subsystem α according to the following equation:

$$p_D = \min\left[1.0,\ \exp\left(\frac{\Delta E_\alpha}{kT}\right)\right] \tag{3}$$

where $\Delta E_\alpha (= E_\alpha^{new} - E_\alpha^{old})$ represents the change in interaction energy in subsystem α caused by the move and kT is the Boltzmann thermal energy. The potential energy in the case of a purely steric interactions for the solute–solute pair and between solute and pore wall can be found in the study of Chun and Phillips (5).

The second random move is a particle interchange between regions α and β. This process is similar to the particle creation and annihilation in the grand canonical μVT ensemble scheme. The probability governing to the transfer of a particle from subsystem α to subsystem β is given as (5):

$$p_T = \min\left[1.0,\ \exp\left\{\ln\left(\frac{N_\alpha V_\alpha}{(N_\beta + 1)V_\alpha}\right) - \frac{\Delta E_\alpha - \Delta E_\beta}{kT}\right\}\right], \tag{4}$$

where N the number of particle and V is the volume of a subsystem.

Fig. 2 shows the computational procedure of the GEMC method used in this study. The random number is generated by the IMSL (7) routines for a random displacement and rotation of particles.

2.2. Non-spherical particles

Rod-like particles, prolate and oblate spheroids, cylinders and hemispheres are the commonly considered axisymmetric non-spherical particles. The rod-like and prolate particles are selected in this study due to the importance and the simplicity of numerical consideration. The behavior of spherical molecules can be characterized by two parameters, a point, equivalent to the center of mass (COM) of molecules, and radius of molecules.

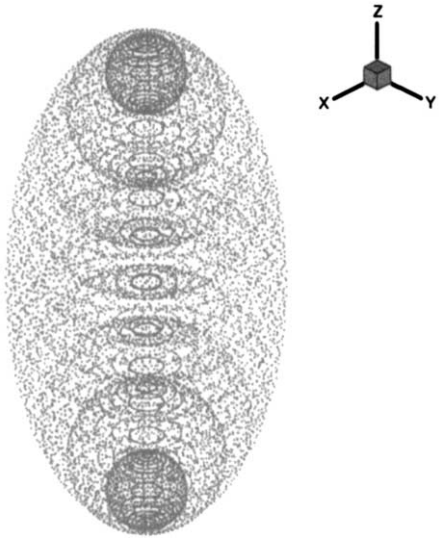

Fig. 3. A prolate spheroid of $\gamma = 2.0$, described by 15 element spheres.

However, the information of orientation is necessary to describe a non-spherical particle as well as COM point and size information. To achieve this, Limbach et al. (2) described particles by the imaginary points on the molecule surface. Molecules were sectioned into appropriate number of equally-spaced discs and each disc was represented by imaginary points along its perimeter. This method is only applicable when a few particles are under consideration. In the case of high concentration solution, hundreds or thousands of particles are used to get the partition coefficients. In this situation, it is almost impossible to simulate by the above method since tremendous computer memory and computation time are required.

In this study, the axisymmetric particles are described by the sphere elements distributed on the particle axis as shown in the Fig. 3. This method dramatically reduces the computational cost because only information of sphere element center positions and radii are necessary for simulations. Forty element spheres are sufficient to describe a prolate spheroid whereas Limbach et al. (2) used up to 762 points on a molecule surface.

The solute-fixed coordinates, (x', y', z') and the space-fixed coordinates, (x, y, z) may be used to characterize the non-spherical particles. Arbitrary particle configurations are quantified by a triple of Eulerian angles giving the orientation of the solute-fixed axes relative to their space-fixed (x, y, z) counterparts. Following the convention of Goldstein (8), the polar and azimuthal angles θ and ϕ determine the orientation of the solute-fixed z' axis as in the usual definition of spherical polar coordinates, and ϕ specifies rotation about this axis. The space-fixed coordinates of a point on the axisymmetric particles with solute-fixed coordinates (x', y', z') centered at (x_0, y_0, z_0) are given by:

$$x = x_0 + (\cos\theta\cos\phi)x' - (\sin\phi)y' + (\sin\theta\cos\phi)z' \quad (5a)$$

$$y = y_0 + (\cos\theta\sin\phi)x' + (\cos\phi)y' + (\sin\theta\sin\phi)z' \quad (5b)$$

$$z = z_0 - (\sin\theta)x' + (\cos\theta)z'. \quad (5c)$$

The rotation angle ϕ does not affect the coordinate transformation since the particles used in this study are axisymmentric.

Based upon the particle describing method using sphere elements, the solute–solute pair potential energy shown in the Eq. (3) can be expressed as:

$$E_{s-s}(d) = \infty, \quad d < h,$$

$$E_{s-s}(d) = 0, \quad d > h, \quad (6)$$

where d is the distance between the j element sphere center position of the i solute and the k element sphere center position of the ip solute, h represents the value of the radius of the j element sphere of the i solute plus the radius of the k element sphere of the ip solute, that is $h = r_{i,j} + r_{ip,k}$. This has to be calculated for all element spheres of the two solutes. Similarly, the potential energy between a solute and the pore wall is given by:

$$E_{s-w}(d) = \infty, \quad d < R_p,$$

$$E_{s-w}(d) = 0, \quad d > R_p, \quad (7)$$

where R_p is the pore radius and d is the farthest distance from the pore centerline to the surface of the i solute. This can be calculated by $d = \rho_{i,j} + r_{i,j}$, where $\rho_{i,j}$ is the distance between the pore centerline and the j element sphere center position of the i solute.

2.3. Computational aspects

A complete cycle of the GEMC simulation used in this study consists of random particle displacements in each region and particle interchange between regions as shown in the Fig. 2. As the initial locations, particles are arranged in face-centered unit lattices in both regions and a number of 800–1300 solute particles enough to preclude the effects of particle numbers, are introduced. Fig. 4 shows initial particle setup when a few particles are introduced. The enough number of element spheres are distributed on the axis of a particle at first, the radii of element spheres are then determined from the contact condition of element spheres and particle surface. If any prolate spheroids, for example, given as:

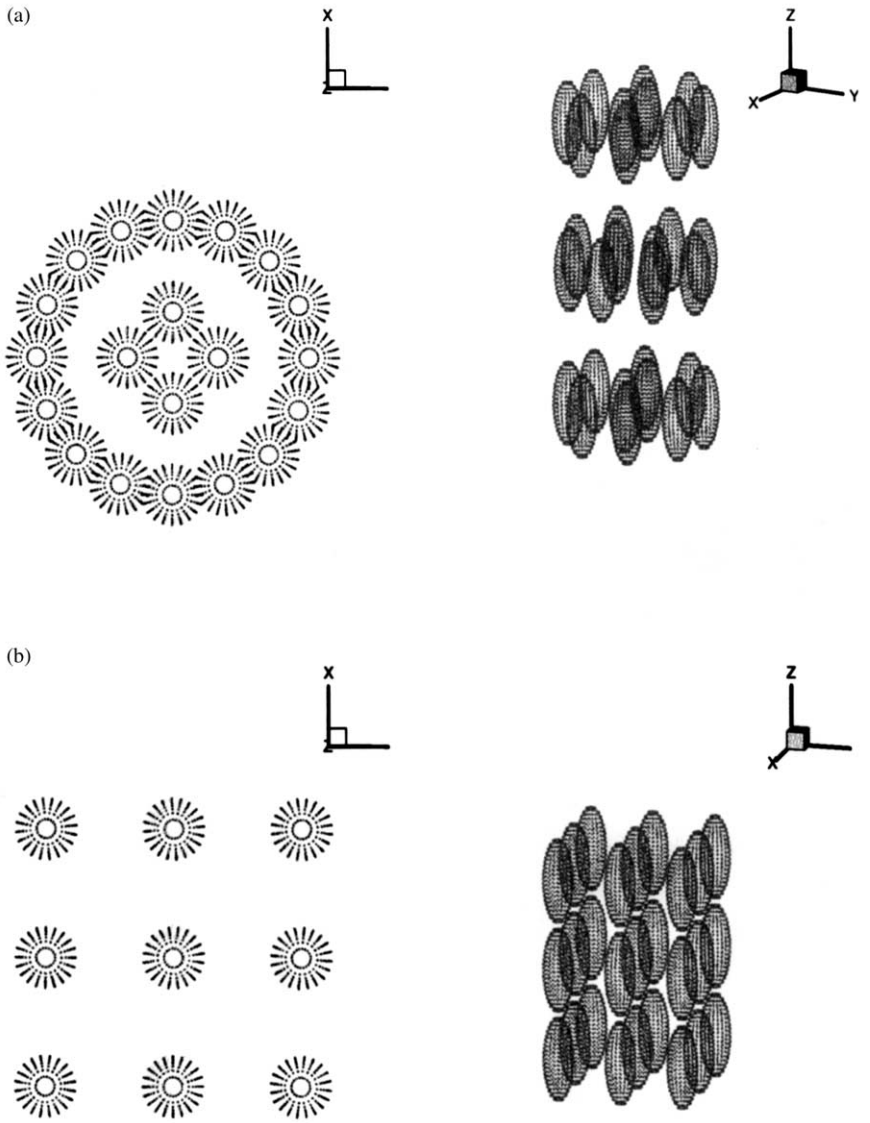

Fig. 4. Examples of initial particle setup, (a) pore region, (b) bulk region.

$$\frac{x'^2}{a^2}+\frac{y'^2}{a^2}+\frac{z'^2}{b^2}=1, \tag{8}$$

the radius of the element sphere located at $z'=k$ is as follow;

$$r_s=\sqrt{\frac{a^2-b^2+k^2}{1-(b/a)^2}}. \tag{9}$$

This condition ensures that any of the element spheres do not exceed the particle surface. A rod-like particle can be represented by aligning element spheres of the same radius on a straight line with pre-determined length. These particle formation processes are performed only one time during the initial particle locations. A random move of non-spherical particles is composed of the two consecutive processes. A particle is translated using the first random number and the polar angle of the

particle is then altered from another random number. Particles after the random movement can be described from the data of element spheres before movement and the Eqs. (5a), (5b) and (5c).

The particles, pore, and bulk unit are non-dimensionalized by the half of the particle length as a characteristic length. To eliminate the effects of the initial distribution of particles, or the non-equilibrium configurations, about $4.8–8.0 \times 10^4$ configurations are discarded and then, the averages are accumulated over the additional $5.0–8.0 \times 10^4$ configurations. The value of the partition coefficient K is checked as a simulation proceeds whether it converges to a well-defined equilibrium value. The number of particles and the size of the pore and unit bulk are adjusted at each simulation to obtain the desired bulk solution concentration. For the radial density profile, the pore cross-section is divided into equal radial increments of shell width, and the number density in radial increment is calculated. The number of element spheres describing particles is adjusted according to the particle shapes and aspect ratios. Typical number of element spheres is 15 and 40 for rod-like and prolate spheroids, respectively.

3. Results and discussion

Giddings et al. (1) developed the equations of the partition coefficients for the several types of non-spherical particles. According to their results and Limbach et al. (2), an analytical expression for infinitely thin rods in circular pores is:

$$K = 1 - \frac{4[(1+\lambda^2)E(\pi/2,\ \lambda) - (1-\lambda^2)F(\pi/2,\ \lambda)]}{3\pi\lambda}, \quad \lambda \le 1 \tag{10a}$$

$$K = 1 - \frac{8}{3\pi}, \quad \lambda = 1 \tag{10b}$$

$$K = 1 - \frac{4[(1+\lambda^2)E(\pi/2,\ \lambda) - (\lambda^2-1)F(\pi/2,\ 1/\lambda)]}{3\pi}, \quad \lambda \ge 1 \tag{10c}$$

where F and E the elliptical integrals of the first and second kind, respectively, and λ is the ratio of the characteristic length, the half axial length of a particle in this study, and the pore radius (b/R_p).

The partition coefficient for spheroids (1,2) is somewhat more complicated and must be evaluated numerically.

$$K = \frac{4}{\pi}\int_0^1 d\alpha \int_0^{\pi/2} d\theta \sin\theta (1-\alpha^2)^{1/2} \times \left[1 - \frac{(\lambda_a^2 - \lambda_b^2)\cos^2\theta + \lambda_b^2}{\{\lambda_a^2\alpha^2 + [(\lambda_a^2 - \lambda_b^2)\cos^2\theta + \lambda_b^2](1-\alpha^2)\}^{1/2}}\right] \times \left[1 - \frac{\lambda_a^2[(\lambda_a^2 - \lambda_b^2)\cos^2\theta + \lambda_b^2]}{\{\lambda_a^2\alpha^2 + [(\lambda_a^2 - \lambda_b^2)\cos^2\theta + \lambda_b^2](1-\alpha^2)\}^{3/2}}\right] \tag{11}$$

where a is the radius of the ellipsoid, b is the half axial length, α is the ratio of a radial coordinate to the ellipsoid radius, λ_a is the ratio of the ellipsoid radius to the pore radius, a/R, λ_b is b/R, and the integrand is taken as zero when either of the multiplicands in parenthesis is negative (2). For later convenience, the aspect ratio is defined as:

$$\gamma = \frac{b}{a}. \tag{12}$$

The partition coefficients from the GEMC simulation for the rod-like particles of the aspect ratio of 2.5 are shown in the Fig. 5. The solid line is for infinitely thin rods according to the analytical results given by the Eqs. (10a), (10b) and (10c), and the symbols are for the present results with the variations of bulk solution concentrations, 5.0, 10.0 and 20.0%. The partition coefficient curves showed rising features for strongly confined spaces with values of λ greater than 0.5 for spherical particles (5). It can be seen from the results of 20.0% that similar rising feature is shown for non-spherical particles.

The partition coefficients of spheres for high concentration are always higher than those of infinite dilute limit. However, some data points

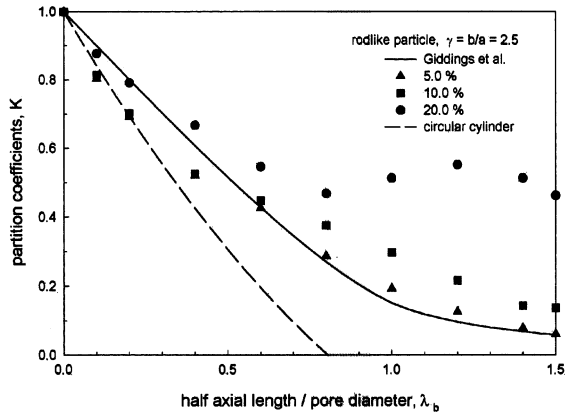

Fig. 5. Partition coefficients K of rod-like particles with aspect ratio, $\gamma = 2.5$ as a function of λ and the variations of bulk concentrations.

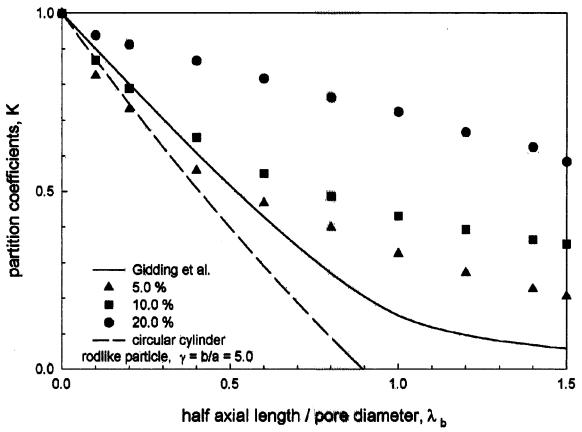

Fig. 6. Partition coefficients K of rod-like particles with aspect ratio, $\gamma = 5.0$ as a function of λ and the variations of bulk concentrations.

at low λ region are less than the analytical results for non-spherical particles as shown in Fig. 6. It is thought to be due to the finite particle length in part and the very low successful particle transfer fractions due to frequent overlap with the pore wall and other particles. The high ratio of the rejection in both insertion and replacement of trials is a common problem in Monte Carlo simulation of the high-density system. The reason why the data points are located under the solid line has to be revealed through the studies of different kind of particles with many cases of aspect ratios. Since the rod-like particle used in this study is finite in essence due to the numerical treatment, it has similarities with a cylinder in shape and behavior. The partition coefficient curve of cylinder for dilute case given by Limbach et al. (2) is also plotted in the Fig. 1 for comparison.

Fig. 6 shows the partition coefficients of rod-like particles according to λ when the aspect ratio is 5.0. The partition coefficients are relatively higher than those of the Fig. 5, corresponds to the aspect ratio of 2.5. The K curve is a nearly straight line when the bulk concentration is 20.0%. It can be seen the effects of aspect ratio is more important for the high λ regions. It is also shown that, from the Figs. 5 and 6, differences are small according to the aspect ratio when the bulk concentration is low. But the differences are remarkable with the variations of aspect ratio when the concentrations are high. This is attributed to the fact that the strong interactions are frequent when the aspect ratio and bulk concentration become high. It can be said that the aspect ratio is important when the bulk solution concentration is high. This result agrees qualitatively with the results of Davidson et al. (9) for the flexible macromolecules between bulk solution and cylindrical pore. According to their Monte Carlo results, the partition coefficients increase when the segment-to-pore size ratio, l/R increases, and the number of mass point of a chain, n decreases. Rod-like particles are considered as chains of which the number of mass point is one. Increasing aspect ratio has the same physical meaning with the increasing of l/R in the case of chains.

Fig. 7 shows the radial density profiles in the pore for the rod-like particles. The concentration profiles are calculated by the two different methods. One is the COM concentration profiles based on the assumption that the whole particle volume is at the particle center. The other is the monomer concentration profile that uses the actual particle volume occupied. The dimensionless concentration is defined as the ratio of a volume concentration of ith shell of a pore, C, to that of the entire pore, C_p. In the case of COM, this can be written as:

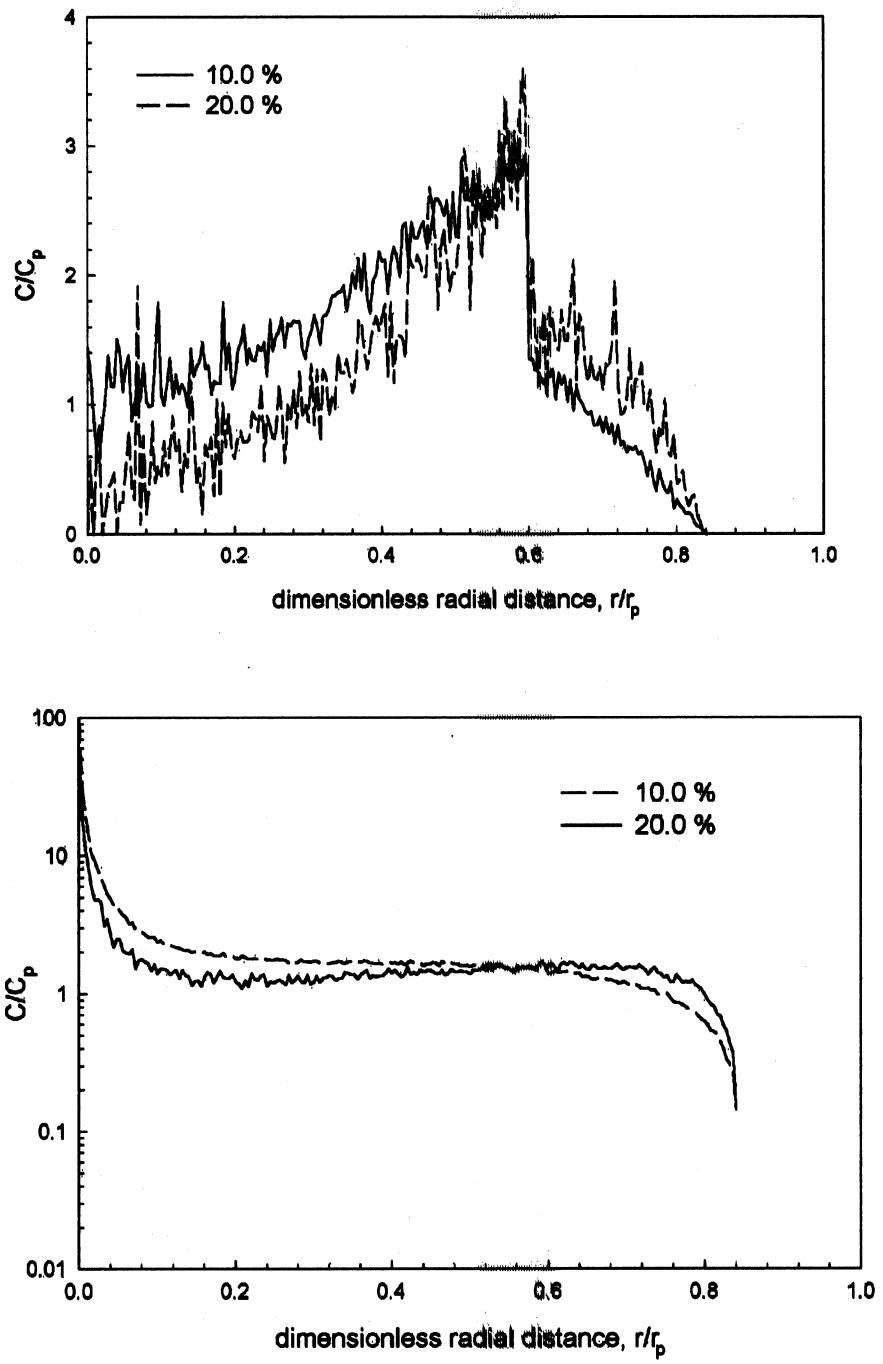

Fig. 7. Density profiles of rod-like particles in the cylindrical pore for $\lambda = 0.4$ and $\gamma = 2.5$, (a) COM concentrations and (b) monomer concentrations.

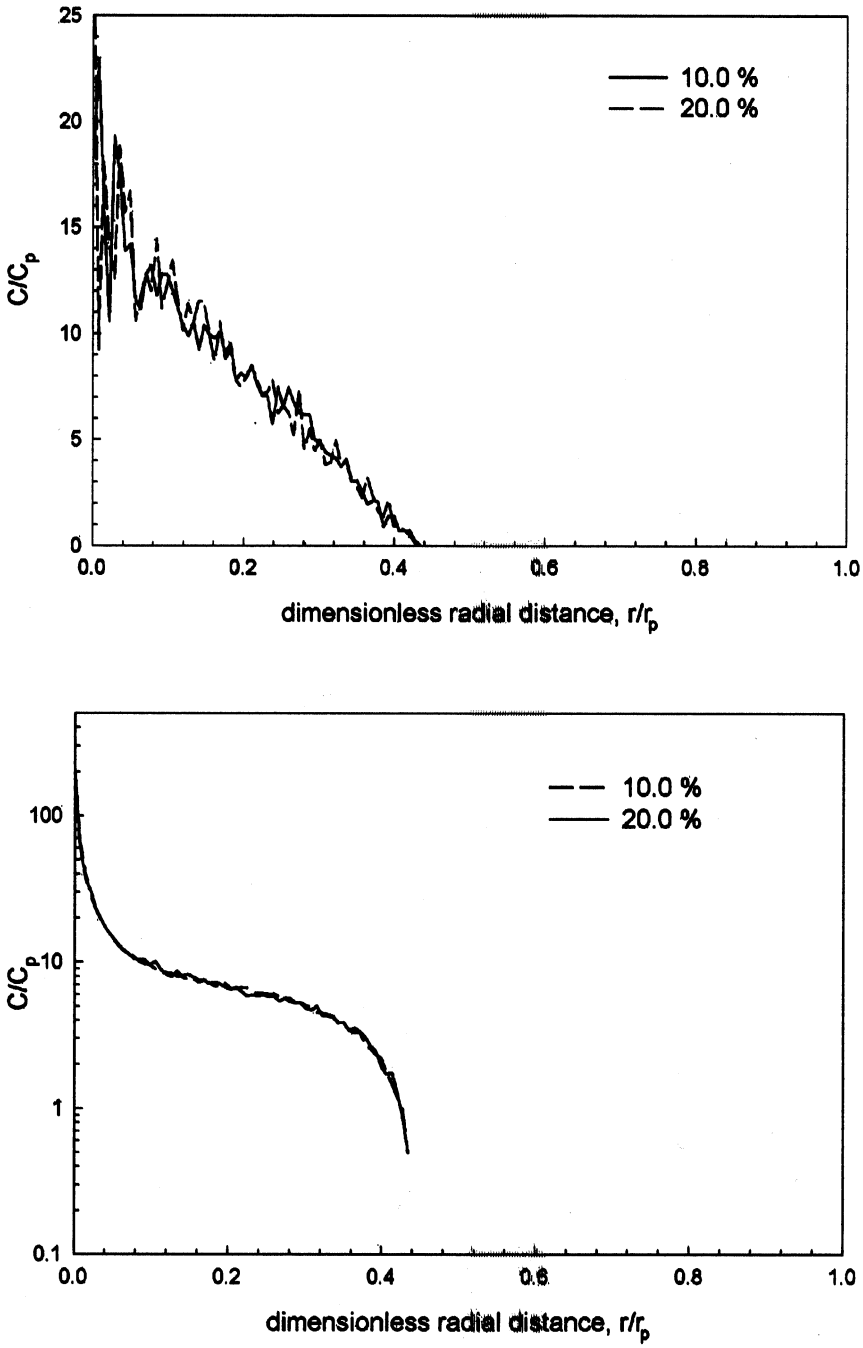

Fig. 8. Density profiles of rod-like particles in the cylindrical pore for $\lambda = 1.4$ and $\gamma = 2.5$, (a) COM concentrations and (b) monomer concentrations.

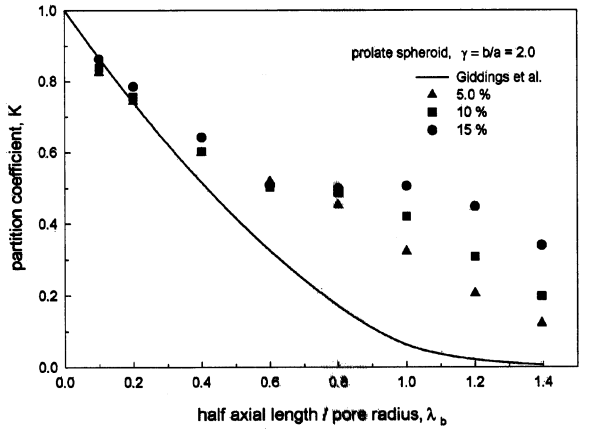

Fig. 9. Partition coefficients K of prolate spheroids with aspect ratio, $\gamma = 2.0$ as a function of λ and the variations of bulk concentrations.

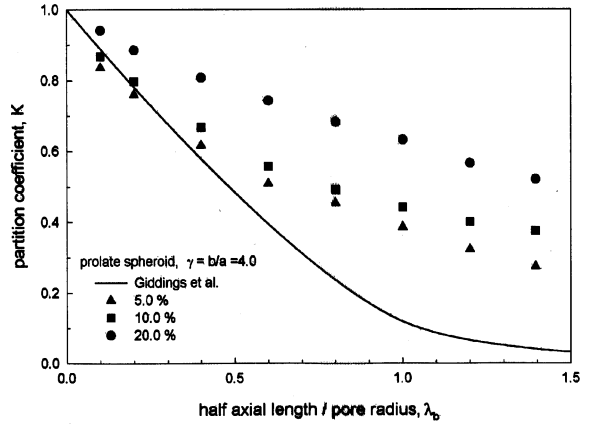

Fig. 10. Partition coefficients K of prolate spheroids with aspect ratio, $\gamma = 4.0$ as a function of λ and the variations of bulk concentrations.

$$\frac{C}{C_p} = \frac{R_p^2}{(R_i^2 - R_{i-1}^2)} \frac{N_i}{N_p}, \tag{13}$$

and for the monomer concentration,

$$\frac{C}{C_p} = \frac{R_p^2}{(R_i^2 - R_{i-1}^2)} \frac{n_t}{N_p n_d}. \tag{14}$$

The N_i and R_i are the number of particles in the ith shell and the inner radius of the ith shell, respectively. The n_d and n_t are the number of element spheres in a particle and the total number of element spheres in the ith shell, respectively.

Fig. 7(a) is the results by the COM method and (b) is by the monomer concentration profiles using the volume of element spheres. It is shown that the concentration in the pore increases according to the radial direction up to 0.6, at a given bulk solution concentration. This is similar to the concentration profiles of uncharged spherical particles. But the results show a discontinuous drop at near the dimensionless radial distance of 0.6 and then the curves decrease slowly. It is attributed to the interaction of particles' two different length scales, the half-length and the radius of a rod-like particle. The COM density profiles have their maximum values at the distance where particles can reach to the pore walls as far as possible by their longitudinal direction and show the discontinuity at this point. The monomer density profiles do not have the discontinuous profile as expected by the physical insights.

Fig. 8(a) and (b) show COM and monomer density profiles for rod-like particles in a cylindrical pore for which $\lambda = 1.4$. A lot of particles are arranged near the center of a pore in the case of highly restricted pores and the number density of particles in a pore show relatively low dependency on the bulk concentrations when compared with the results of low λ values.

The partition coefficients for prolate spheroids with aspect ratios of 2.0 and 4.0 are shown in Figs. 9 and 10, respectively. The partition coefficient, K increases with increasing of bulk concentrations and aspect ratios. The rising feature similar to the sphere solute at high λ regions can be noted when the aspect ratio, $\gamma = 2.0$. When aspect ratio, γ is 4.0, there is no significant rising feature at the K values and forms a nearly straight line when bulk concentration is high compared with the previous figure. It is shown that from the comparison of Figs. 9 and 10, bulk concentrations become more important when aspect ratio is large.

Figs. 11 and 12 show density profiles for prolate spheroids and rod-like particles in cylindrical pores for which $\lambda = 0.2$ and $\lambda = 0.6$, respectively. The COM density profiles for the two particle shapes change abruptly at the point where it is

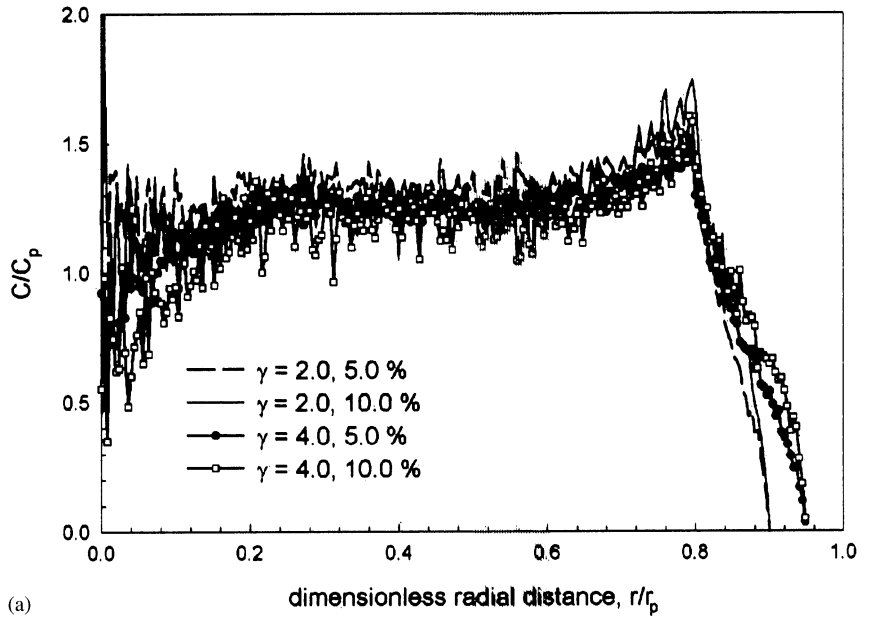

(a)

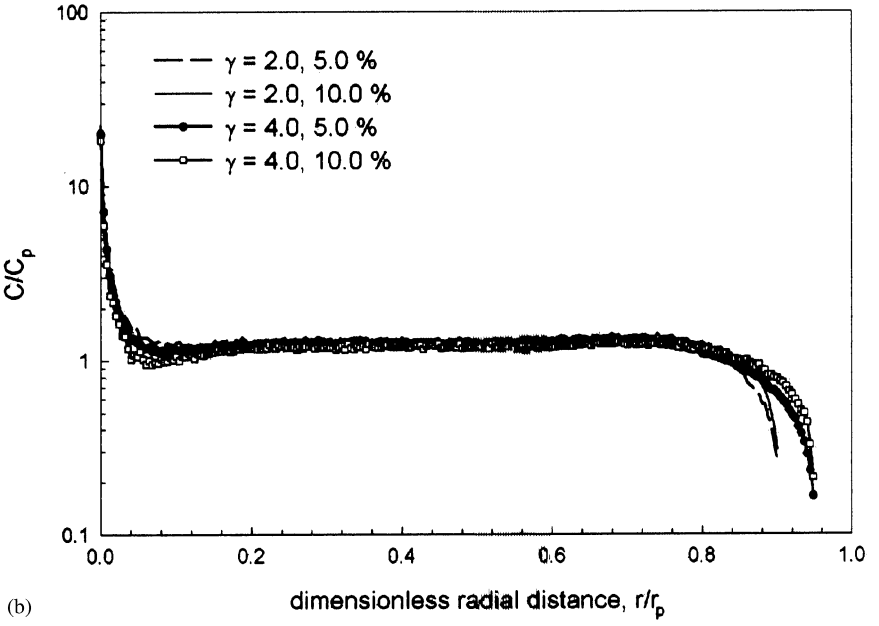

(b)

Fig. 11. Density profiles of prolate spheroids at various conditions in the cylindrical pore for $\lambda = 0.2$ according to the radial direction, (a) COM concentration profiles, (b) monomer concentration profiles.

equal to the normalized particle characteristic length, b/R_p. For example, rod-like particles shown in the Fig. 12, pore radius is 1.667 for obtaining $\lambda = 0.6$ when the particle half-length b is 1.0, and these give the maximum dimensionless radial value of 0.4 that particle can reach the pore

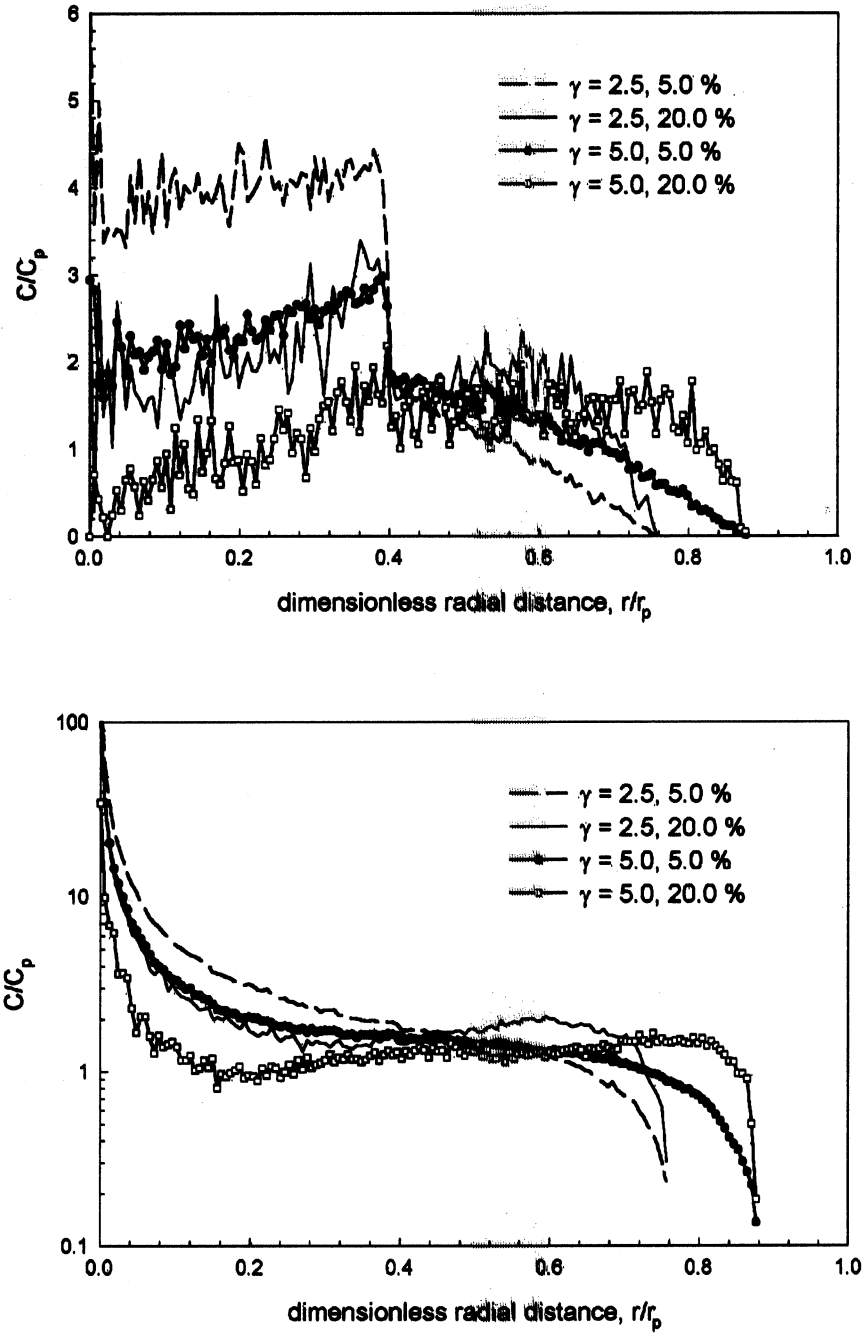

Fig. 12. Density profiles of rod-like particles at various conditions in the cylindrical pore for $\lambda = 0.6$ according to the radial direction, (a) COM concentration profiles, (b) monomer concentration profiles.

wall by its longitudinal direction. The density curves in the pore reach its maximum value at this point and then decrease abruptly. Particles can interact with pore wall only by their radial direction (a in Eq. (6)) at the outer region from the point.

Note that the density profiles at the inner part of the discontinuous point of the pore are high when the bulk concentrations are low. This fact differs from the case of sphere molecules. At the outer region of the pore, the density curves for the high bulk concentrations are located above than that of low bulk concentration. If the bulk concentration is the same, as aspect ratio becomes high, that is, for longer particles, the density in the inner region of the discontinuous point becomes lower, but it goes higher in the outer region. This is thought to be that the aspect ratio of the particles is high, the particles are aligned with the axis of a pore. The monomer concentration profiles, calculated by the actual particle volume, show smooth decrease near to the pore walls. This difference is due to the assumption for calculating the COM density profile such that the volume of a particle lies at the center of the particles.

4. Conclusions

Density profiles and partition coefficients for rod-like particles and prolate spheroids in cylindrical pores have been studied by stochastic GEMC method. This study shows that it is possible to analyze the partitioning behavior of non-spherical particles of high concentration by the GEMC method, which is difficult to obtain by analytical methods. Non-spherical particles are described by the sphere elements and the computational time is remarkably saved by the method. This method is also efficient to calculate the concentration profiles.

The COM density profiles obtained by the GEMC simulations show the discontinuity near the pore wall. But the characteristics of the curves differ from each other according to the particle shapes. The partition coefficient, K increases with increasing of the aspect ratios in general. The partition coefficient curves show the rising feature as the bulk concentration becomes high and this is similar to the sphere solutes. But the aspect ratio becomes large in a high bulk concentration solution, the rising feature disappears and the K curve is a nearly straight line.

An extension of the calculations presented here to account for the characteristics of non-spherical particles, such as hemisphere, oblate spheroid, and disc, should be studied consecutively. The systems of charged, non-spherical particles and pores should also be studied to accounting for electrostatic effects on equilibrium partitioning.

Acknowledgements

This work was made possible in part by the support of the Korea Institute of Science and Technology.

References

1. J.C. Gidding, E. Kucera, C.P. Russel, M.N. Myers, J. Phys. Chem. 72 (1968) 4397.
2. K.W. Limbach, J.M. Nitsche, J. Wei, AIChE J. 35 (1989) 42.
3. J.M. Nitsche, K.W. Limbach, Ind. Eng. Chem. Res. 33 (1994) 1391.
4. D.A. McQuarrie, Statistical Mechanics, Harper and Row, New York, 1976.
5. M.S. Chun, R.J. Phillips, AIChE J. 43 (1997) 1194.
6. M.P. Allen, D.J. Tildesley, Computer Simulation of Liquids, Oxford University Press, New York, 1987.
7. IMSL Math Libraries, Visual Numerics Inc.
8. H. Goldstein, Classical Mechanics, Addison–Wesley, Cambridge, MA, 1950.
9. M.G. Davidson, U.W. Suter, W.M. Deen, Macromolecules 20 (1987) 1141.